

# SuperQuadricOcc: Multi-Layer Gaussian Approximation of Superquadrics for Real-Time Self-Supervised Occupancy Estimation

Seamie Hayes, Reenu Mohandas, Tim Brophy, Alexandre Boulch, Ganesh Sistu, Ciaran Eising

**Abstract**—Semantic occupancy estimation enables comprehensive scene understanding for automated driving, providing dense spatial and semantic information essential for perception and planning. While Gaussian representations have been widely adopted in self-supervised occupancy estimation, the deployment of a large number of Gaussian primitives drastically increases memory requirements and is not suitable for real-time inference. In contrast, superquadrics permit reduced primitive count and lower memory requirements due to their diverse shape set. However, implementation into a self-supervised occupancy model is nontrivial due to the absence of a superquadric rasterizer to enable model supervision. Our proposed method, SuperQuadricOcc, employs a superquadric-based scene representation. By leveraging a multi-layer icosphere-tessellated Gaussian approximation of superquadrics, we enable Gaussian rasterization for supervision during training. On the Occ3D dataset, SuperQuadricOcc achieves a 75% reduction in memory footprint, 124% faster inference, and a 5.9% improvement in mIoU compared to previous Gaussian-based methods, without the use of temporal labels. To our knowledge, this is the first occupancy model to enable real-time inference while maintaining competitive performance. The use of superquadrics reduces the number of primitives required for scene modeling by 84% relative to Gaussian-based approaches. Finally, evaluation against prior methods is facilitated by our fast superquadric voxelization module. The code will be released as open source.

## I. INTRODUCTION

The application of computer vision to scene understanding has gained significant traction, particularly in perception for automated vehicles, which focuses on estimating dynamic and complex driving environments. Initially, 3D object detection served as the foundation for spatial understanding, providing precise localization of agents in the scene [2]. However, its cuboid prediction space limits the representation of irregular objects, such as bicycles. Bird’s Eye View (BEV) later emerged as a top-down fixed-grid prediction approach offering broader scene coverage [3], but its lack of vertical

This publication has emanated from research conducted with the financial support of Taighde Éireann – Research Ireland under Grant number 18/CRT/6049. For the purpose of Open Access, the author has applied a CC BY public copyright licence to any Author Accepted Manuscript version arising from this submission.

Seamie Hayes and Ciarán Eising are with the Department of Electronic and Computer Engineering, the Research Ireland Centre for Research Training in Foundations in Data Science, and the Data Driven Computer Engineering (D<sup>2</sup>ICE) Research Centre, all hosted in the University of Limerick, Limerick, V94 T9PX Ireland.

Reenu Mohandas, Tim Brophy, and Ganesh Sistu are with the Department of Electronic and Computer Engineering, and the Data Driven Computer Engineering (D<sup>2</sup>ICE) Research Centre, University of Limerick, Limerick, V94 T9PX, Ireland.

Alexandre Boulch is with valeo.ai, 75008 Paris, France.

Corresponding author: Seamie Hayes (e-mail: seamie.hayes@ul.ie)

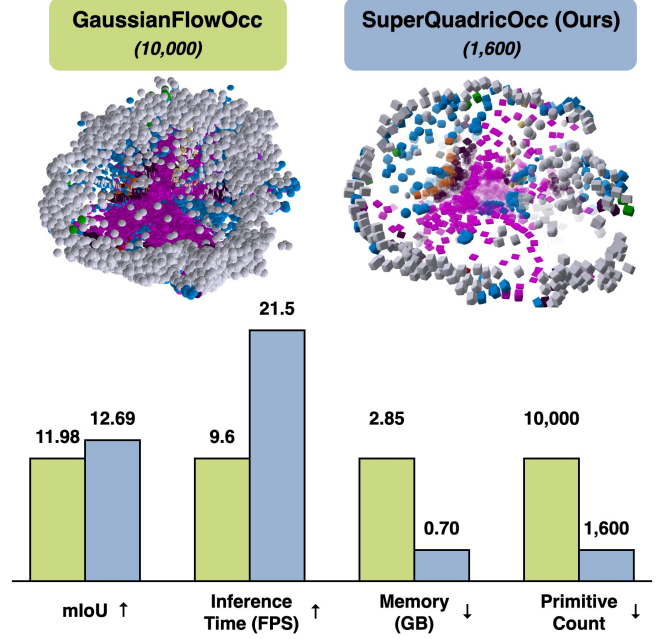


Fig. 1: **Comparison of GaussianFlowOcc [1] and our model, SuperQuadricOcc:** Replacing Gaussians with superquadrics enables more efficient scene modeling through a sparser and more expressive representation. Our method achieves higher mIoU, faster inference, and lower memory consumption with significantly fewer primitives. Ground truth is provided in Figure 4.

reasoning restricted comprehensive 3D understanding, thus limiting real-world applicability. Semantic occupancy estimation addressed this by extending BEV into 3D, representing the world as a discretized voxel grid.

Within semantic occupancy estimation, scene representation has evolved from dense voxel-based formats to more efficient Gaussian representations, and most recently, to superquadrics [4]; however, superquadrics have not yet been explored in the self-supervised setting. Self-supervised occupancy models rely on 2D pseudo-labels derived from Visual Foundation Models (VFM), such as Grounded-SAM [5]–[7] for semantic information and Metric3Dv2 [8] for depth cues, eliminating the need for dense manual annotations [9]–[11]. Given the discrepancy between the 2D supervision space and the 3D evaluation space, neural rendering methods such as NeRF [12] and Gaussian Splatting [13] are well-suited for bridging this gap. Nonetheless, challenges remain, including reliance on large foundation models such as Metric3Dv2

during inference to address depth ambiguity [9], and the need for thousands of Gaussian primitives to model fine details [1]. Both factors increase inference time and memory requirements, hindering real-time deployment.

In an effort to achieve real-time inference, we introduce the self-supervised occupancy model SuperQuadricOcc. Our approach employs superquadrics for scene representation, leveraging their diverse shape set to model objects more compactly than previous Gaussian-based methods. This design reduces the number of primitives required for scene modeling by 84% compared to GaussianFlowOcc [1]. For efficient and effective supervision against 2D labels, we apply a multi-layer Gaussian approximation to each superquadric primitive, enabling Gaussian rasterization as a proxy for rendering the superquadric distribution.

Incorporating temporal labels for adjacent renderings, as done in GaussianFlowOcc [1], improves evaluation metrics by enhancing view consistency. However, we omit this component in our model and in GaussianFlowOcc for comparison, as it more than triples the training time. As illustrated in Figure 1, superquadrics model the scene more sparsely yet provide a richer and more structured representation compared to Gaussians. This translates directly into improved efficiency and accuracy. SuperQuadricOcc achieves a 12.69 mean Intersection over Union (mIoU) on the Occ3D-nuScenes dataset [14], marking a 5.9% improvement over GaussianFlowOcc. Additionally, due to the compact scene representation, our model attains real-time inference at 21.5 FPS. Memory usage is also significantly reduced, requiring only 0.70 GB during inference, a 75% reduction. By exploiting the efficiency of superquadrics, our model delivers real-time inference with strong performance, establishing a foundation for future research in superquadric-based occupancy estimation.

The contributions of this paper are summarized as follows:

- **SuperQuadric Scene Representation:** We present SuperQuadricOcc, the first self-supervised semantic occupancy estimation model to employ superquadrics for scene representation.
- **Multi-Layer Gaussian Approximation:** We introduce the use of 3D Gaussians to approximate the occupancy probability of superquadrics for neural rendering, enabling efficient supervision during training.
- **Real-Time Inference:** SuperQuadricOcc increases inference time by 124% to achieve 21.5 FPS, enabling real-time deployment, while also lowering memory consumption by 75%. We achieve 12.69 mIoU on the Occ3D-nuScenes dataset.

## II. RELATED WORKS

### A. Semantic Occupancy Prediction

Semantic occupancy estimation can generally be categorized into two main approaches: supervised and self-supervised. Both approaches aim to estimate voxel-level semantics in a discretized 3D environment. Supervised occupancy estimation has seen significant growth with the introduction of standardized datasets [14]–[18], which provide occupancy labels for major benchmark datasets such

as Waymo [19], nuScenes [20], and KITTI [21]. Scene representation relies on voxel-based structure largely due to the voxel-based evaluation space [22]–[26]. However, alternative representations have emerged, including cylindrical-coordinate formats [27], octree-based structures [28], and, more recently, Gaussian representations [29]–[32]. Gaussian scene representation has become particularly popular due to its reduced memory requirements compared to dense voxel grids [29], and its compatibility with Gaussian rasterization, which enables additional loss computation [33], [34] for view consistency, improving overall scene understanding. Furthermore, Gaussian rasterization has been integrated into voxel-based models as a supplementary loss through voxel-to-Gaussian conversion modules [23], [35]–[38].

In self-supervised models, Gaussian scene representations are particularly advantageous due to this research domain’s reliance on 2D labels for supervision [1], [9], [10]. GaussianOcc first demonstrated this by extending OccNeRF [11], replacing the NeRF renderer with Gaussian splatting; however, both approaches suffer from high memory consumption due to their voxel-based structures. GaussTR [9] introduced a foundation model-style framework, incorporating VFMs such as Talk2DINO [39], CLIP [40], Metric3Dv2 [8], and DINOv2 [41], achieving state-of-the-art performance. Nonetheless, its reliance on Metric3Dv2 during inference and inefficient voxelization techniques limits real-time applicability. GaussianFlowOcc [1] further advanced prior work by introducing a temporal flow module for improved view consistency and induced attention for faster and more effective interactions between Gaussian features. However, the use of 10,000 Gaussian primitives substantially increases inference time, again preventing real-time performance. Furthermore, incorporating temporal labels via the temporal flow module triples training time and is therefore omitted from our experiments.

Our proposed approach, SuperQuadricOcc, resolves these limitations by employing a superquadric-based scene representation, yielding a significantly sparser model that utilizes only 1600 superquadric primitives. This design enables real-time inference, marking a first in the field of occupancy estimation. Through efficient supervision using our multi-layer Gaussian approximation for superquadric rendering, we achieve state-of-the-art performance in both inference speed and memory efficiency.

### B. SuperQuadrics for Scene Modelling

Superquadrics were first introduced and parameterized by Alan H. Barr [42] as a unified mathematical framework for applications in computer graphics and numerical methods for 3D design. In computer vision, superquadrics have been widely adopted for scene modeling, particularly in 3D reconstruction [43]–[47] and static scene reconstruction [48], where neural rendering techniques are often used to provide supervision.

Paschalidou *et al.* [45] proposed representing 3D shapes as compositions of superquadrics rather than cuboids. The model is trained in an unsupervised manner using a bidi-

rectional Chamfer distance between points sampled from predicted superquadric surfaces and ground-truth occupancy reconstructions. PartGS [46] and GaussianBlock [47] further extended this approach, drawing inspiration from prior work that places Gaussians on mesh surfaces for rendering [49], [50]. Both methods approximate the superquadric surface by positioning Gaussians on a deformed icosphere whose vertices lie on the surface of the superquadric. In PartGS, both the Gaussians and superquadric geometry are jointly optimized, while in GaussianBlock, the superquadric primitives are first learned via differentiable rendering and later enhanced with bound Gaussians for high-fidelity rendering and editing. SuperDec [48] fits superquadrics to point cloud data using a Point-Voxel CNN and a transformer decoder to predict superquadric parameters.

The use of superquadrics in supervised occupancy estimation was first explored in QuadricFormer [4], which outperforms the Gaussian-based GaussianFormer [29] in evaluation metrics while reducing inference time and memory consumption. In our model, SuperQuadricOcc, we extend this concept to self-supervised occupancy estimation, marking the first application of superquadrics in this setting. For model supervision, we adopt the icosphere tessellation strategy from PartGS [46] and GaussianBlock [47], approximating the superquadric surface with Gaussians. Since we model superquadrics as occupancy probabilities, we further this approach by introducing a multi-layer Gaussian formulation to effectively capture the underlying distribution.

### III. METHODOLOGY

In this section, we outline our superquadric-based occupancy framework, SuperQuadricOcc. We define the occupancy prediction problem (Sec. III-A), describe the formulation of superquadrics and their occupancy probability (Sec. III-B), and present the model architecture (Sec. III-C). We then detail the superquadric-to-Gaussian module for supervision (Sec. III-D) and the superquadric voxelization module for efficient inference (Sec. III-E). The overall model architecture is shown in Figure 2.

#### A. Problem Statement

Semantic occupancy estimation discretizes 3D space into a voxel grid indexed by  $\mathbb{Z}^3$ , where each voxel is assigned a semantic label from classes  $C = \{c_0, c_1, \dots, c_n\}$ , defined as  $V : \mathbb{Z}^3 \rightarrow C$ . Predictions are generated from  $N$  calibrated multi-view images at time  $t$ ,  $I_t = \{I_t^1, I_t^2, \dots, I_t^N\}$ , with the model output  $V_t = F(I_t)$ . Previous self-supervised methods used intermediate voxel grids or 3D Gaussian representations for scene understanding, whereas our approach models the scene directly with superquadrics.

#### B. SuperQuadrics

For each sample, a set of  $N$  superquadric primitives  $S = \{S_1, S_2, \dots, S_N\}$  is used to represent the scene. Each superquadric shares the same set of parameters as Gaussians: mean  $\mu \in \mathbb{R}^3$ , scale  $s \in \mathbb{R}^3$ , quaternion rotation  $r \in \mathbb{R}^4$ ,

opacity  $\sigma \in \mathbb{R}^1$ , and semantic logits  $c \in \mathbb{R}^C$ , with two additional parameters  $\varepsilon_1, \varepsilon_2 \in \mathbb{R}$ :

$$S = \{\mu, s, \sigma, c, \varepsilon_1, \varepsilon_2\} \quad (1)$$

As described by Barr [42], the  $\varepsilon$  parameters control the squareness and roundness of the shape:  $\varepsilon_1$  governs squareness along the north-south direction, while  $\varepsilon_2$  does so along the east-west direction. The inside-outside function,  $f$ , for a superquadric is defined as:

$$f(\mathbf{x}) = \left( \left( \frac{x}{s_x} \right)^{\frac{2}{\varepsilon_2}} + \left( \frac{y}{s_y} \right)^{\frac{2}{\varepsilon_2}} \right)^{\frac{\varepsilon_2}{\varepsilon_1}} + \left( \frac{z}{s_z} \right)^{\frac{2}{\varepsilon_1}} \quad (2)$$

where  $\mathbf{x} = (x, y, z)^T$  and  $\mathbf{s} = (s_x, s_y, s_z)^T$ . Following Zuo *et al.* [4], the occupancy probability of a superquadric can be formulated as follows. To evaluate a point  $\mathbf{x}$  for a given superquadric  $S$ , it is first transformed into the local coordinate system of the superquadric via rotation and translation to obtain  $\mathbf{x}_S$ :

$$\mathbf{x}_S = R(\mathbf{x} - \mu) \quad (3)$$

The superquadric occupancy probability at point  $\mathbf{x}$  is then expressed as:

$$p_o = e^{-f(\mathbf{x}_S)} \quad (4)$$

This formulation is employed during training prior to rendering and during inference for voxelization.

#### C. Model Architecture

Our model architecture is based on GaussianFlowOcc, excluding the temporal module to enable a direct comparison between Gaussian and superquadric-based occupancy estimation. The overall architecture is illustrated in Figure 2. Image features  $\hat{I}$  are extracted from six surround-view camera images using a ResNet-50 backbone. Superquadric feature vectors  $S_F \in \mathbb{R}^{N \times C}$  and superquadric means  $S_M \in \mathbb{R}^{N \times 3}$  are randomly initialized and subsequently refined within 3 subsequent blocks of the Transformer network.

The Transformer network incorporates both temporal and self-attention mechanisms to enhance the superquadric features  $S_F$ . To improve efficiency, an induced attention mechanism is used, which reduces memory usage and facilitates more effective learning through the condensed representation of the superquadric features. Deformable attention over image features enables the extraction of rich semantic and depth cues.

The refined superquadric features  $S_F$  are passed through five lightweight MLPs to predict the remaining superquadric properties  $\{s, \sigma, c, \varepsilon_1, \varepsilon_2\}$ . For efficient supervision during training, we employ a superquadric-to-Gaussian module that performs a multi-layer icosphere-tessellated Gaussian approximation of each superquadric for Gaussian rasterization.

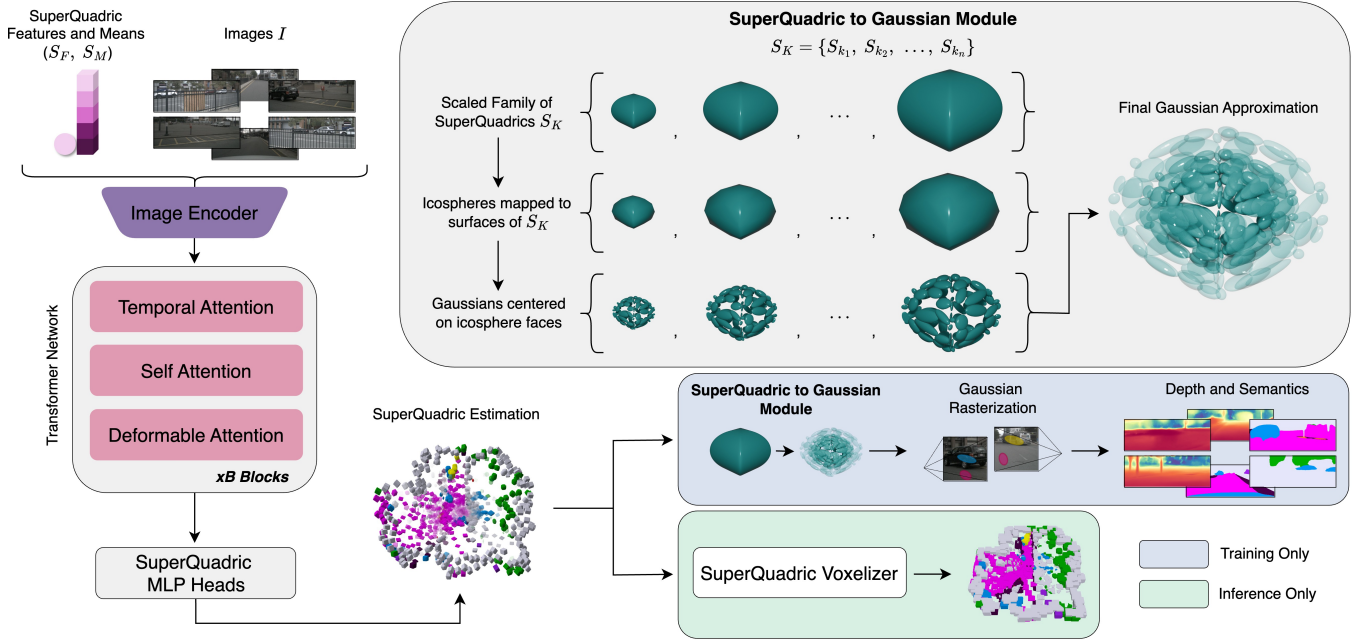


Fig. 2: **Architecture of SuperQuadricOcc:** The model extracts image features and refines learnable superquadric features and means in the *Transformer Network*, similar to GaussianFlowOcc [1]. The MLP prediction heads estimate the remaining superquadric properties:  $\{s, \sigma, c, \varepsilon_1, \varepsilon_2\}$ . During training, the *SuperQuadric to Gaussian Module* generates a multi-layer Gaussian approximation per superquadric for rendered supervision, while during inference, the *SuperQuadric Voxelizer* efficiently produces voxel labels for evaluation.

#### D. SuperQuadric to Gaussian Module

To enable rendering of superquadrics, we adopt a multi-layer Gaussian approximation. Previous works approximated only the surface of superquadrics using 2D Gaussians for 3D modeling [46], [47]. In contrast, since our formulation treats superquadrics as occupancy probabilities, we extend this approach with a multi-layer approximation using 3D Gaussians.

Given a superquadric  $S = (s, \varepsilon_1, \varepsilon_2)$ , we augment its scale parameters with positive scalars  $K = \{k_1, k_2, \dots, k_n\} \subset \mathbb{R}^+$  to define a scaled family of superquadrics:

$$S_K = \{S(k, s, \varepsilon_1, \varepsilon_2) \mid k \in K\} \quad (5)$$

We approximate each occupancy distribution of the scaled superquadrics following established frameworks for Gaussian placement on mesh surfaces [46], [47]. For each  $S_k \in S_K$ , a tessellated unit icosphere is constructed, with vertices lying on the surface of a unit sphere. Each vertex on the icosphere, defined by spherical coordinates  $(\eta, \omega)$ , is mapped to the superquadric surface through signed powers of trigonometric functions, controlled by  $\varepsilon_1$  and  $\varepsilon_2$ . This produces a mesh within the superquadric that approximates its surface. Icospheres with a higher vertex count yield a more accurate approximation of the superquadric surface at the cost of additional computation. Gaussians are then centered on each face center and oriented along the surface normal and tangent directions, with their  $xy$  scales proportional to the local face area. This is performed so that each Gaussian sufficiently covers the area of each face. Each Gaussian inherits the

semantics of its parent superquadric. For Gaussian opacity, we deviate from prior formulations, which assign the opacity of each Gaussian to that of the parent superquadric, and we instead assign it to be:

$$\sigma_{\text{gauss}} = \sigma \cdot e^{f(\mathbf{m})} \quad (6)$$

where  $\sigma$  denotes the opacity of the superquadric and  $\mathbf{m}$  is the Gaussian mean. This scaling aligns the Gaussian density with that of the superquadric, ensuring that the density evaluated at the Gaussian's center exactly matches the corresponding point within the superquadric distribution.

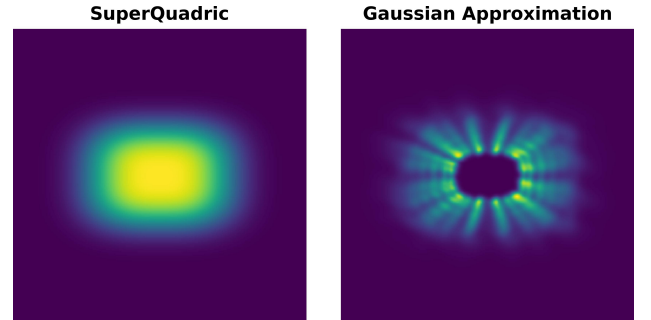


Fig. 3: **SuperQuadric and Gaussian Distribution:** 2D slice showing a superquadric density and its Gaussian approximation from the superquadric-to-Gaussian module. Parameters:  $s = (1.0, 0.7, 0.5)$ ,  $\varepsilon_1 = 0.6$ ,  $\varepsilon_2 = 0.7$ ,  $K \subset [0.5, 2.5]$ .

To more accurately capture the occupancy distribution, we extend Gaussians into 3D by introducing an additional

$z$ -scale parameter along each local normal direction. For a Gaussian center  $\mathbf{x}_k$  sampled on  $S_k$ , we define a corresponding Gaussian  $\mathbf{x}_{k+1}$  on  $S_{k+1}$  at the same angular coordinates  $(\eta, \omega)$ . The Euclidean distance between  $\mathbf{x}_k$  and  $\mathbf{x}_{k+1}$  defines the local normal extent, and we assign half this distance as the Gaussian  $z$ -scale:

$$s_z(\eta, \omega) = \frac{1}{2} \|\mathbf{x}_{k+1}(\eta, \omega) - \mathbf{x}_k(\eta, \omega)\|. \quad (7)$$

This implementation enables each Gaussian to decay along its normal direction, thereby better approximating the superquadric occupancy density. An illustration of our multi-layer Gaussian approximation is shown in Figure 3. The Gaussians are well-positioned in each layer through the parametric mapping from the icosphere to the superquadric surface. The density values remain accurate due to the adaptive  $z$ -scale in Equation (7) and the opacity scaling in Equation (6). Interior layers are absent because the scale values are restricted to a minimum of 0.5, as further discussed in our ablation study in Table VI.

While this approximation is not analytically exact, since Gaussians decay quadratically in the exponent, whereas superquadrics follow a power-law decay governed by  $(\varepsilon_1, \varepsilon_2)$ , it provides a reliable basis for supervision. During training, this module serves Gaussian rasterization to render semantic and depth maps for supervision using 2D pseudo-labels, following standard practice in self-supervised models.

#### E. SuperQuadric Voxelization

To enable direct comparison with previous state-of-the-art methods, we develop a superquadric voxelization module for evaluation. Following the procedure of Boeder *et al.* [1], we voxelize opacity and semantics separately, to obtain the following formulation:

$$v_o(\mathbf{p}; S) = \sum_{i \in N(v)} \exp(-f_i(\mathbf{p}_s)) \sigma_i \quad (8)$$

$$v_c(\mathbf{p}; S) = \sum_{i \in N(v)} \exp(-f_i(\mathbf{p}_s)) c_i \quad (9)$$

For each voxel  $v$  with center  $\mathbf{p}$  in the discretized grid, we aggregate contributions from all superquadrics  $S$  within its neighborhood  $N = 5$ , similar to GaussianFlowOcc [1]. Each superquadric is then transformed into the local coordinate frame of the voxel using Equation (3) to obtain  $\mathbf{p}_s$ . The contribution is computed using the weighted sums of the occupancy probability function defined in Equation (4). Voxels below a defined opacity threshold  $\tau$ , are assigned as free in the semantic voxel to obtain the final prediction. We assign  $\tau = 0.01$ , through empirical tuning.

### IV. EXPERIMENTS

#### A. Datasets and Metrics

We evaluate our method on the Occ3D-nuScenes [14] and OpenOcc [17] datasets, comparing performance against state-of-the-art models. For both datasets, the voxel evaluation space spans  $[-40, 40]$  along the  $X$  and  $Y$  axes,

and  $[-1, 5.4]$  along the  $Z$  axis, with a voxel resolution of  $0.4m^3$ . Evaluation metrics include Intersection over Union (IoU), which measures binary voxel classification as free or occupied, and mIoU, which computes IoU per semantic class, reflecting semantic understanding. We also evaluate performance using the Ray Intersection over Union (RayIoU) metric [52]. Inference speed and memory consumption are also reported, with all models evaluated on a single NVIDIA A100 GPU.

#### B. Implementation

For a fair comparison with GaussianFlowOcc [1], we train our model following their experimental configuration. We use a ResNet-50 backbone with an input image resolution of  $256 \times 704$  and adopt their Gaussian Transformer network comprising three blocks. Induced attention is implemented with 500 inducing points. Our approach employs 1600 superquadric primitives, compared to the 10,000 Gaussians used in GaussianFlowOcc. In the superquadric-to-Gaussian module, we use an 80-faced icosahedron with scale values:  $K = [0.5, 0.6, 0.75, 0.9, 1.05, 1.2, 1.6, 2.0, 2.5]$ , forming an  $S_{K=9}$  scaled family of superquadrics. This results in 720 Gaussians per superquadric for rendering. All models are trained for 18 epochs on 4 NVIDIA A100 GPUs with a batch size of 6.

#### C. Main Results

In this section, we present the main results of our model compared to GaussianFlowOcc on the Occ3D-nuScenes [14] and OpenOcc [17] datasets. Table I reports various results on Occ3D, where our model surpasses the Gaussian-based GaussianFlowOcc, achieving a 5.9% increase in mIoU while utilizing 84% fewer primitives. When GaussianFlowOcc is trained with an equivalent number of primitives (1600), performance drops by 16.7% in mIoU compared to its 10,000-Gaussian configuration. This highlights the spatial expressiveness of superquadrics due to their diverse shape parameterization. However, we observe a reduction in IoU relative to GaussianFlowOcc, likely caused by a slight overdensification resulting from a mismatch between the Gaussian loss representation and the superquadric evaluation representation. Furthermore, SuperQuadricOcc outperforms GaussianFlowOcc on dynamic object detection, particularly for vulnerable road users, showing a +3.84 IoU improvement for the bicyclist class. This gain stems from the irregular shapes of such objects, which are better captured by the flexible geometry of superquadrics. Although GaussTR [9] achieves higher mIoU, this is attributed to its use of foundation models during inference, which significantly degrades its inference speed, limiting its applicability for real-time systems.

In terms of inference speed, our model reaches state-of-the-art real-time performance at 21.5 FPS, representing a 124% improvement over the 10,000-Gaussian GaussianFlowOcc model. Compared to GaussTR, we achieve a 7066% increase in inference speed, attributed to the absence of foundation models at inference and an efficient

TABLE I: **Occupancy Estimation results on the Occ3D-nuScenes [14] dataset:** Rep. denotes the method of scene representation: Gauss - Gaussian; Quad - SuperQuadric. Mem. denotes the memory (GB) required for a single sample inference. GaussianFlowOcc results are reproduced locally without the deployment of temporal labels. GaussianFlowOcc\* denotes the equivalent trained model with 1,600 Gaussians. The best-performing results between the GaussianFlowOcc models and SuperQuadricOcc only are highlighted in **bold**. Other state-of-the-art models are included for reference.

Model	Rep.	Mem.	FPS	IoU	mIoU	barrier	bicycle	bus	car	const. veh.	motorcycle	pedestrian	traffic cone	trailer	truck	drive. surf.	sidewalk	terrain	manmade	vegetation
SelfOcc [51]	Voxel	3.00	7.4	45.01	10.54	0.15	0.66	5.46	12.54	0.00	0.80	2.10	0.00	0.00	8.25	55.49	26.30	26.54	14.22	5.60
OcNeRF [11]	Voxel	12.68	5.4	46.43	10.81	0.83	0.82	5.13	12.49	3.50	0.23	3.10	1.84	0.52	3.90	52.62	20.81	24.75	18.45	13.19
GaussianOcc [10]	Voxel	11.81	5.4	42.91	11.26	1.79	5.82	14.58	13.55	1.30	2.82	7.95	9.76	0.56	9.61	44.59	20.10	17.58	8.61	10.29
GaussTR [9]	Gauss	1.97	0.3	44.54	13.76	6.50	8.54	21.77	24.27	6.26	15.48	7.94	1.86	6.10	17.16	36.98	17.21	7.16	21.18	9.99
GaussianFlowOcc [1]	Gauss	2.85	9.6	<b>35.85</b>	11.98	5.48	1.85	9.26	9.41	0.33	1.88	3.00	3.03	1.51	7.32	<b>57.77</b>	<b>22.26</b>	<b>28.25</b>	13.59	14.72
GaussianFlowOcc* [1]	Gauss	<b>0.62</b>	20.4	35.40	9.98	3.20	1.60	8.06	7.40	1.18	2.51	2.14	1.93	1.77	6.09	47.34	19.90	22.52	13.22	10.88
SuperQuadricOcc (Ours)	Quad	0.70	<b>21.5</b>	33.67	<b>12.69</b>	<b>5.78</b>	<b>5.69</b>	<b>16.32</b>	<b>13.06</b>	<b>3.72</b>	<b>5.69</b>	<b>3.94</b>	<b>3.54</b>	<b>2.56</b>	<b>11.94</b>	43.58	20.66	24.15	<b>14.45</b>	<b>15.29</b>

voxelization module. Furthermore, our model maintains a compact footprint of 0.70 GB, slightly higher than the 1600-Gaussian GaussianFlowOcc model, which uses less memory but achieves a lower mIoU, indicating our approach offers a better performance–efficiency balance. Compared to voxel-based approaches, our method reduces memory consumption by 94% due to the sparse nature of the superquadric representation.

TABLE II: **RayIoU evaluated on the Occ3D-nuScenes [14] dataset:** GaussianFlowOcc\* denotes the model trained with 1,600 Gaussians. The best-performing model for each evaluation metric is highlighted in **bold**.

Model	RayIoU	RayIoU@1	RayIoU@2	RayIoU@4
GaussianFlowOcc [1]	10.38	6.49	10.01	14.65
GaussianFlowOcc* [1]	9.69	5.79	9.40	13.88
SuperQuadricOcc (Ours)	<b>10.93</b>	<b>6.62</b>	<b>10.70</b>	<b>15.49</b>

TABLE III: **RayIoU evaluated on the OpenOccv2 [14] dataset:** GaussianFlowOcc\* denotes the model trained with 1,600 Gaussians. The best-performing model for each evaluation metric is highlighted in **bold**.

Model	RayIoU	RayIoU@1	RayIoU@2	RayIoU@4
GaussianFlowOcc [1]	11.86	<b>7.78</b>	11.61	16.19
GaussianFlowOcc* [1]	10.71	6.64	10.48	15.01
SuperQuadricOcc (Ours)	<b>12.46</b>	<b>7.78</b>	<b>12.29</b>	<b>17.30</b>

We also evaluate GaussianFlowOcc and our model on RayIoU across the Occ3D and OpenOcc datasets, as presented in Tables II and III, respectively. Consistent with earlier observations, our superquadric-based model achieves higher RayIoU scores than the Gaussian-based baseline across all benchmarks. SuperQuadricOcc experiences a 5.3% and a 5.1% increase compared to the 10,000-Gaussian GaussianFlowOcc model, respectively.

#### D. Ablation Studies

To analyze the impact of different design choices in our model, particularly those related to the superquadric-to-Gaussian module, we conduct a series of ablation studies.

**Ablation on Primitive Count:** In Table IV, we compare GaussianFlowOcc and our model across varying primitive counts. We observe that at lower primitive counts, our model substantially outperforms GaussianFlowOcc, for instance, with 1200 primitives, SuperQuadricOcc achieves a 65% higher mIoU. However, at higher primitive counts exceeding approximately 2000, GaussianFlowOcc begins to outperform SuperQuadricOcc. This may stem from issues in the loss computation, as the model tends to learn smaller-scale superquadrics, which can interfere with the superquadric-to-Gaussian conversion process, leading to inaccurate Gaussian placement due to reduced scale. Nevertheless, our 1600-primitive SuperQuadricOcc model still surpasses the 10,000-Gaussian GaussianFlowOcc model, demonstrating the efficiency and representational capacity of superquadrics.

TABLE IV: **Ablation of Number of Primitives:** Evaluated on the mIoU metric. The best result overall is highlighted in **bold**.

Primitive Count	GaussianFlowOcc	SuperQuadricOcc (Ours)
1200	7.53	12.44
1600	9.98	<b>12.69</b>
2000	10.37	12.70
5000	12.50	6.95
10000	11.98	4.59

**Ablation on Icosphere Faces:** Table V investigates the number of faces per scaled superquadric in the superquadric-to-Gaussian module, which is initialized by a ‘level’ parameter. Results show that using 80 faces per scaled superquadric achieves the best balance, providing sufficient surface coverage without excessive computational overhead, as seen with 320 faces. Using 20 faces may also be considered optimal, as it results in only a 0.03 decrease in mIoU while reducing training time. Notably, configurations with 1280 faces result in an out-of-memory (OOM) error, even with a batch size of 1.

**Ablation on Scale Values:** Table VI examines the effect of different scale values for the scaled family of superquadrics,  $S_K$ . We find that scale configurations emphasizing interior layers of the superquadric yield better performance, as these regions exhibit higher density. For example, using a fixed

TABLE V: **Ablation on Icosphere Faces:** OOM denotes out-of-memory. The best result is highlighted in **bold**.

Level	Faces	mIoU
0	20	12.66
1	80	<b>12.69</b>
2	320	12.29
3	1280	OOM

scale difference of 0.2 yields worse results, again due to insufficient emphasis on interior layers. In contrast, overemphasizing interior or exterior layers leads to degraded results, likely due to sparser sampling and a mismatch between Gaussian and superquadric density distributions.

TABLE VI: **Ablation on Scale values:** The best result overall is highlighted in **bold**.

Scale Values	mIoU
[0.5, 0.6, 0.75, 0.9, 1.05, 1.2, 1.6, 2.0, 2.5]	<b>12.69</b>
[0.1, 0.22, 0.40, 0.58, 0.76, 0.94, 1.42, 1.90, 2.5]	12.37
[0.5, 0.65, 0.88, 1.1, 1.33, 1.55, 2.15, 2.75, 3.5]	12.19
[0.5, 0.7, 0.9, 1.1, 1.3, 1.5, 1.7, 1.9, 2.1, 2.3, 2.5]	12.50

**Ablation on Scaling of Gaussian Opacity:** Table VII evaluates the effect of including the superquadric scaling term,  $e^{f(\mathbf{m})}$ , in the Gaussian opacity formulation of Equation 6. Including this term improves results by allowing Gaussians to more accurately approximate the superquadric distribution, producing a better-aligned supervision signal.

TABLE VII: **Ablation on Scaling of Gaussian Opacity:** The best result is highlighted in **bold**.

Scale Opacity	mIoU
✓	<b>12.69</b>
✗	8.23

**Ablation on Gaussian Z-scale:** Table VIII studies the effect of the Gaussian z-scale formulation from Equation (7). Assigning the z-scale as half the Euclidean distance to corresponding Gaussians yields higher performance than using a constant scale. Similar to the opacity scaling ablation, this provides a more faithful density distribution within the superquadric, resulting in improved supervision quality.

TABLE VIII: **Ablation on Gaussian Z-scale:** The best result is highlighted in **bold**.

Z-Scale	mIoU
0.01	12.60
0.1	11.32
Half-Euclidean	<b>12.69</b>

### E. Visualizations

Figure 4 presents visual comparisons between SuperQuadricOcc and the 10,000- and 1600-Gaussian versions

of GaussianFlowOcc on two validation samples. Corresponding primitives are also visualized. SuperQuadricOcc effectively leverages the diverse shape set of superquadrics, modeling cubes, cuboids, and ellipsoids, which is particularly advantageous for planar regions such as roads. In contrast, the 1600-Gaussian GaussianFlowOcc model struggles to represent objects such as vehicles accurately, consistent with results in Table I. The Gaussian-based model requires a much higher number of primitives to match the spatial fidelity achieved by our approach, demonstrating the efficiency of superquadrics for holistic scene modeling. All models exhibit difficulty in densely populated scenes, such as the bottom scene, which contains multiple vehicles, often overcompensating by initializing excess primitives in likely occupied regions.

Zooming in on the car (blue) and traffic cone (yellow) for the respective samples, SuperQuadricOcc produces more accurate predictions. For the car, GaussianFlowOcc fails to capture the shape precisely, underestimating it in the 1,600-Gaussian model and overestimating it in the 10,000-Gaussian model. For the case of the traffic cone, SuperQuadricOcc more accurately localizes the cones, consistent with the results in Table I.

## V. CONCLUSION

In conclusion, this paper presents a comprehensive exploration of superquadrics for scene representation in perception for automated vehicles through our proposed model, SuperQuadricOcc. The model introduces a self-supervised occupancy estimation framework utilizing a multi-layer superquadric-to-Gaussian module, which effectively approximates the superquadric probability distribution to enable rendering. Our results demonstrate that superquadrics provide a significantly more compact yet accurate representation of scenes, even when compared to Gaussian-based models employing over six times the number of primitives. SuperQuadricOcc achieves a 5.9% increase in mIoU and 75% reduced memory consumption compared to GaussianFlowOcc, highlighting the enhanced representational efficiency of superquadrics for complex and diverse environments. Furthermore, SuperQuadricOcc achieves real-time inference at 21.5 FPS, made possible by the reduced primitive count and the efficiency of our superquadric-to-occupancy module. For future work, we plan to extend SuperQuadricOcc by incorporating temporal labels and exploring a NeRF-based renderer to compare against our Gaussian rendering approach. Overall, the findings indicate that superquadrics offer a promising direction for further optimization in 3D scene understanding and semantic occupancy estimation.

## APPENDIX

### A. Semantic Occupancy

In Figure 5, we provide additional visual analysis of the predicted semantic occupancy and corresponding superquadrics for several samples. Our model performs well on dynamic objects such as cars and buses, but struggles to complete large static structures like the road, consistent

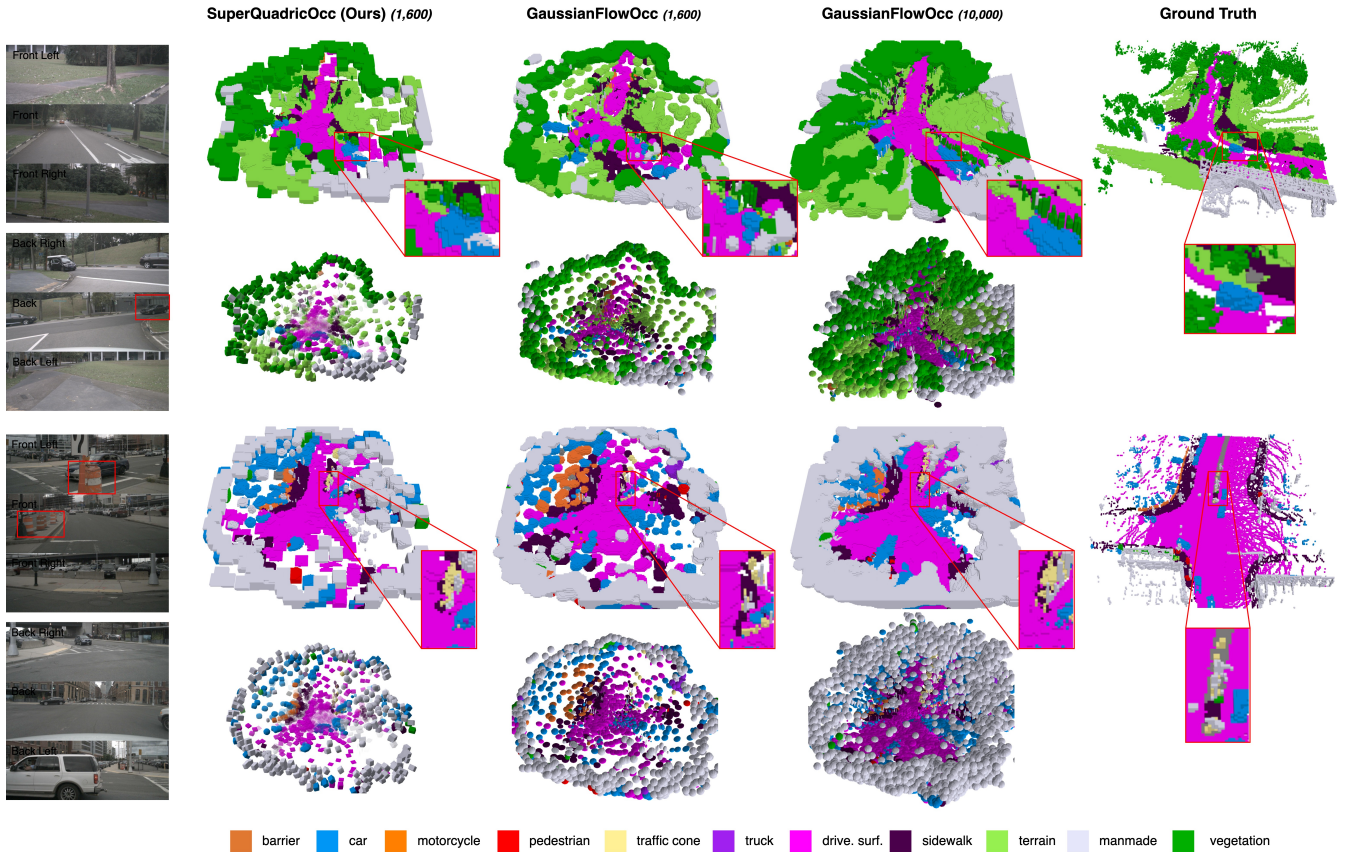


Fig. 4: **Visualization of Primitives and Voxel Estimation:** Comparison between SuperQuadricOcc and the 10,000- and 1600-GaussianFlowOcc models on the Occ3D-nuScenes dataset [14] for sample tokens edde57e6dfefb416e936d9056824b8253 and 135bf33890ba4ca2984a931444923eda.

with the main results table. This limitation may be addressed by initializing larger-scale superquadric primitives for static objects than for dynamic ones.

Furthermore, we provide videos comparing the occupancy predictions of SuperQuadricOcc with those of the 1600- and 10,000-Gaussian GaussianFlowOcc models [1], alongside ground truth, for three scenes: scene-0016, scene-0092, and scene-0276. Consistent with earlier analysis, SuperQuadricOcc produces superior predictions due to its diverse shape set, particularly when compared with the 1600-Gaussian GaussianFlowOcc.

### B. Depth and Semantic Renders

Figure 6 shows rendered semantic and depth maps for SuperQuadricOcc compared with the GaussianFlowOcc models. In the semantic renders, SuperQuadricOcc provides improved predictions for partially occluded objects, such as the pedestrian in the front-right image and the car in the back-right image. However, the model misclassifies the car in the front-right view as a truck, despite correctly identifying its wheels. This may result from mislabeled ground-truth data, with a similar misclassification observed in the 1600-Gaussian model. For depth rendering, SuperQuadricOcc demonstrates more accurate geometric predictions, notably for the car in the front-right view and the pole in the

back-right image, compared to 10,000-Gaussian GaussianFlowOcc. Nonetheless, our model occasionally predicts a superquadric in the sky region of the camera back image, likely an artifact of the superquadric-to-Gaussian conversion process. The same artifact is also observed in the 1,600-Gaussian model.

Furthermore, we provide additional visualizations of the rendered depth and semantics for two more samples of SuperQuadricOcc in Figure 7. The semantic renders show strong segmentation of vehicles and challenging objects such as poles, as seen in the back-right view of the top sample. Depth estimation is also accurate, with objects predicted at appropriate distances.

### REFERENCES

- [1] S. Boeder, F. Gigengack, and B. Risse, “Gaussianflowocc: Sparse and weakly supervised occupancy estimation using gaussian splatting and temporal flow,” *arXiv preprint arXiv:2502.17288*, 2025.
- [2] J. Mao, S. Shi, X. Wang, and H. Li, “3d object detection for autonomous driving: A comprehensive survey,” *International Journal of Computer Vision*, vol. 131, no. 8, pp. 1909–1963, 2023.
- [3] Y. Ma, T. Wang, X. Bai, H. Yang, Y. Hou, Y. Wang, Y. Qiao, R. Yang, and X. Zhu, “Vision-centric bev perception: A survey,” *IEEE Transactions on Pattern Analysis and Machine Intelligence*, 2024.
- [4] S. Zuo, W. Zheng, X. Han, L. Yang, Y. Pan, and J. Lu, “Quadricformer: Scene as superquadrics for 3d semantic occupancy prediction,” *arXiv preprint arXiv:2506.10977*, 2025.

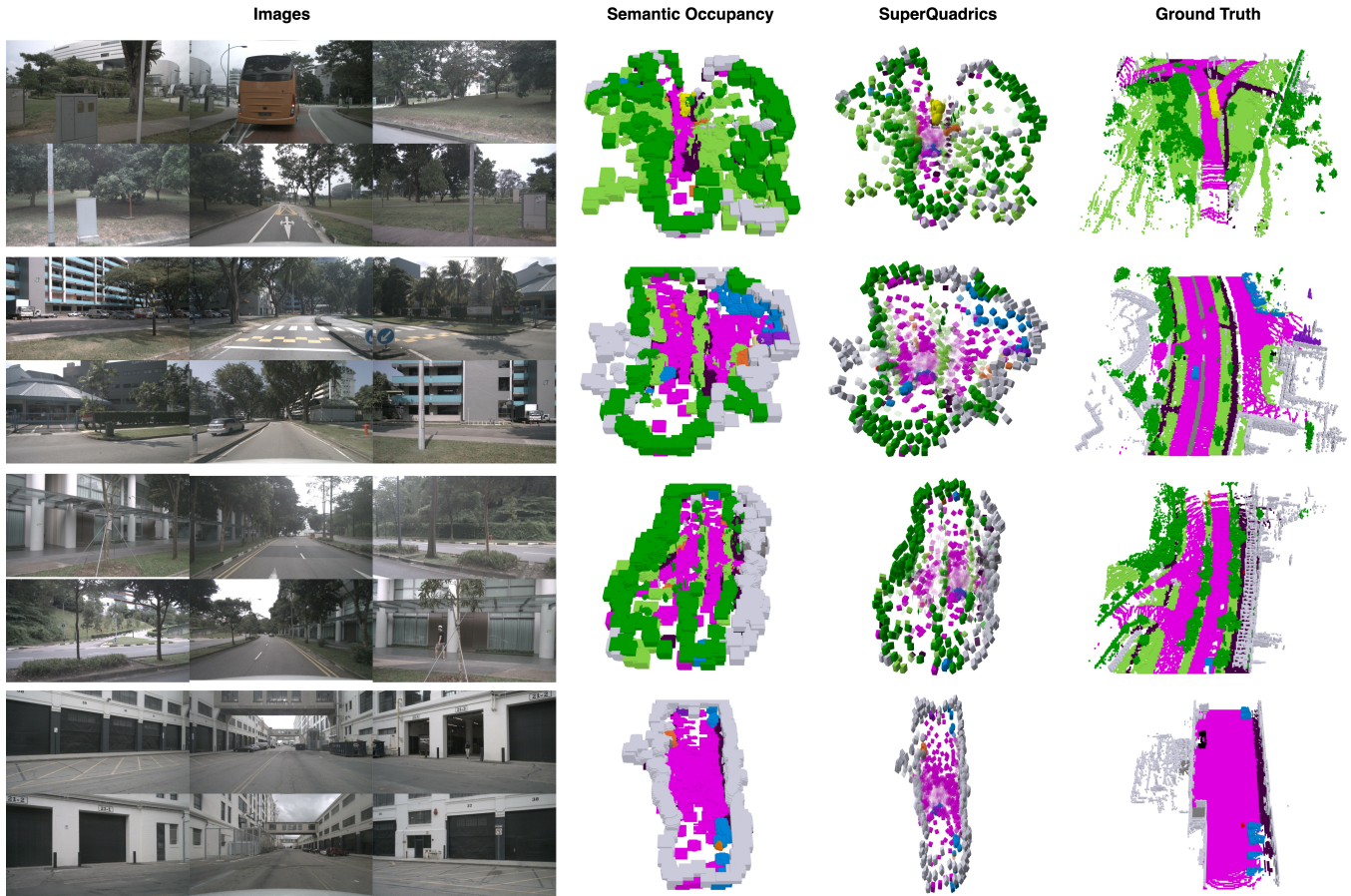


Fig. 5: **Additional Visualizations:** Images, predicted semantic occupancy, superquadric primitives, and ground truth voxels visualized. For sample tokens 43cfc03be6f842ae8942c995f8e3f2fb. 997e5e6c149d4bbcb3c210335f901c3d. d21bdfbca9f4edaa4bf4f54fffa6f4b. 6b10154e2b3146ab85b43f3cfe053d6d.

- [5] T. Ren, S. Liu, A. Zeng, J. Lin, K. Li, H. Cao, J. Chen, X. Huang, Y. Chen, F. Yan *et al.*, “Grounded sam: Assembling open-world models for diverse visual tasks,” *arXiv preprint arXiv:2401.14159*, 2024.
- [6] A. Kirillov, E. Mintun, N. Ravi, H. Mao, C. Rolland, L. Gustafson, T. Xiao, S. Whitehead, A. C. Berg, W.-Y. Lo *et al.*, “Segment anything,” in *Proceedings of the IEEE/CVF international conference on computer vision*, 2023, pp. 4015–4026.
- [7] S. Liu, Z. Zeng, T. Ren, F. Li, H. Zhang, J. Yang, Q. Jiang, C. Li, J. Yang, H. Su *et al.*, “Grounding dino: Marrying dino with grounded pre-training for open-set object detection,” in *European conference on computer vision*. Springer, 2024, pp. 38–55.
- [8] M. Hu, W. Yin, C. Zhang, Z. Cai, X. Long, H. Chen, K. Wang, G. Yu, C. Shen, and S. Shen, “Metric3d v2: A versatile monocular geometric foundation model for zero-shot metric depth and surface normal estimation,” *IEEE Transactions on Pattern Analysis and Machine Intelligence*, 2024.
- [9] H. Jiang, L. Liu, T. Cheng, X. Wang, T. Lin, Z. Su, W. Liu, and X. Wang, “Gausstr: Foundation model-aligned gaussian transformer for self-supervised 3d spatial understanding,” in *Proceedings of the Computer Vision and Pattern Recognition Conference*, 2025, pp. 11 960–11 970.
- [10] W. Gan, F. Liu, H. Xu, N. Mo, and N. o Yokoya, “Gaussianocc: Fully self-supervised and efficient 3d occupancy estimation with gaussian splatting,” *CoRR*, vol. abs/2408.11447, 2024. [Online]. Available: <https://doi.org/10.48550/arXiv.2408.11447>
- [11] C. Zhang, J. Yan, Y. Wei, J. Li, L. Liu, Y. Tang, Y. Duan, and J. Lu, “Occnerf: Self-supervised multi-camera occupancy prediction with neural radiance fields,” *CoRR*, 2023.
- [12] B. Mildenhall, P. P. Srinivasan, M. Tancik, J. T. Barron, R. Ramamoorthi, and R. Ng, “Nerf: Representing scenes as neural radiance fields for view synthesis,” *Communications of the ACM*, vol. 65, no. 1, pp. 99–106, 2021.
- [13] B. Kerbl, G. Kopanas, T. Leimkühler, and G. Drettakis, “3d gaussian splatting for real-time radiance field rendering,” *ACM Trans. Graph.*, vol. 42, no. 4, pp. 139–1, 2023.
- [14] X. Tian, T. Jiang, L. Yun, Y. Mao, H. Yang, Y. Wang, Y. Wang, and H. Zhao, “Occ3d: A large-scale 3d occupancy prediction benchmark for autonomous driving,” *Advances in Neural Information Processing Systems*, vol. 36, pp. 64 318–64 330, 2023.
- [15] Y. Wei, L. Zhao, W. Zheng, Z. Zhu, J. Zhou, and J. Lu, “Surroundocc: Multi-camera 3d occupancy prediction for autonomous driving,” in *Proceedings of the IEEE/CVF International Conference on Computer Vision*, 2023, pp. 21 729–21 740.
- [16] X. Wang, Z. Zhu, W. Xu, Y. Zhang, Y. Wei, X. Chi, Y. Ye, D. Du, J. Lu, and X. Wang, “Openoccupancy: A large scale benchmark for surrounding semantic occupancy perception,” in *Proceedings of the IEEE/CVF International Conference on Computer Vision*, 2023, pp. 17 850–17 859.
- [17] C. Sima, W. Tong, T. Wang, L. Chen, S. Wu, H. Deng, Y. Gu, L. Lu, P. Luo, D. Lin *et al.*, “Scene as occupancy,” *arXiv preprint arXiv:2306.02851*, 2023.
- [18] Y. Li, S. Li, X. Liu, M. Gong, K. Li, N. Chen, Z. Wang, Z. Li, T. Jiang, F. Yu *et al.*, “Sscbench: A large-scale 3d semantic scene completion benchmark for autonomous driving,” in *2024 IEEE/RSJ International Conference on Intelligent Robots and Systems (IROS)*. IEEE, 2024, pp. 13 333–13 340.
- [19] P. Sun, H. Kretschmar, X. Dotiwalla, A. Chouard, V. Patnaik, P. Tsui, J. Guo, Y. Zhou, Y. Chai, B. Caine *et al.*, “Scalability in perception for autonomous driving: Waymo open dataset,” in *Proceedings of the IEEE/CVF conference on computer vision and pattern recognition*, 2020, pp. 2446–2454.

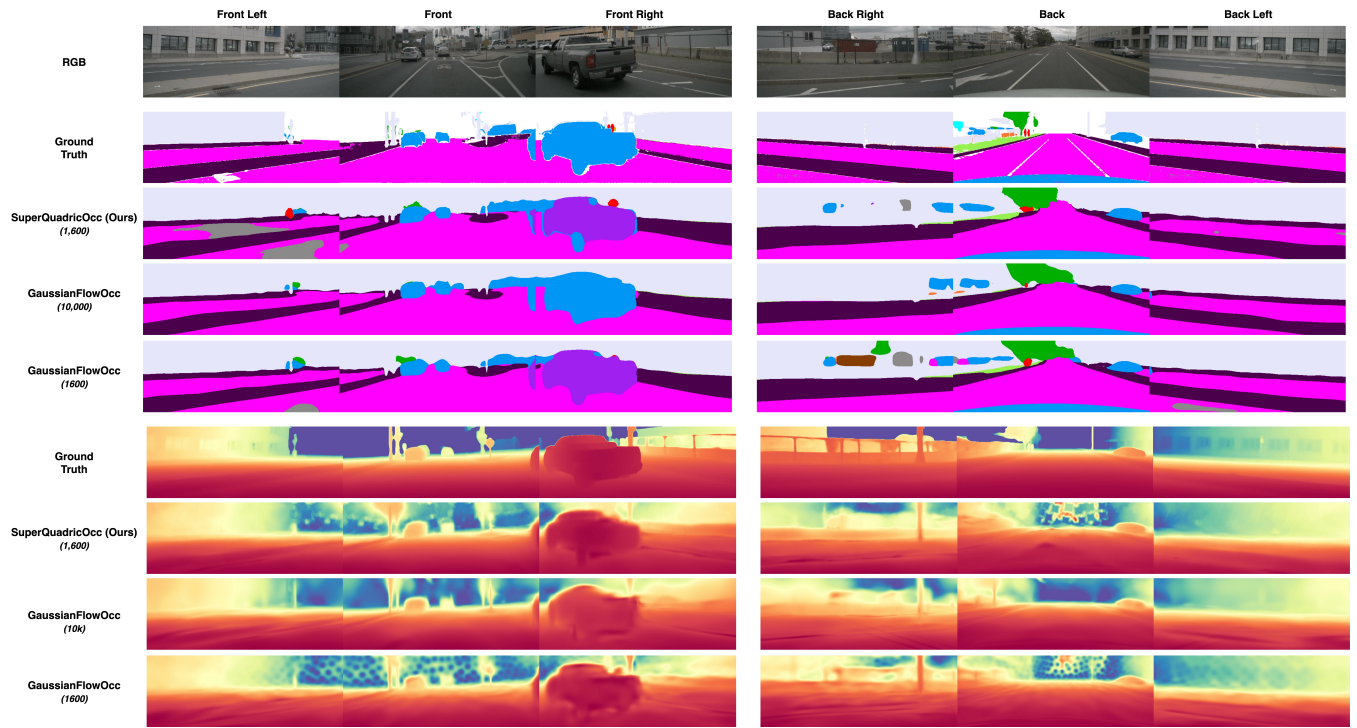


Fig. 6: **Visualization of Rendered Semantics and Depth:** Comparison of semantic and depth renderings produced by SuperQuadricOcc and 10,000-GaussianFlowOcc on the Occ3D-nuScenes dataset [14] for sample token 05cf2a68a2cf4ff1838034f8ecae0c82.

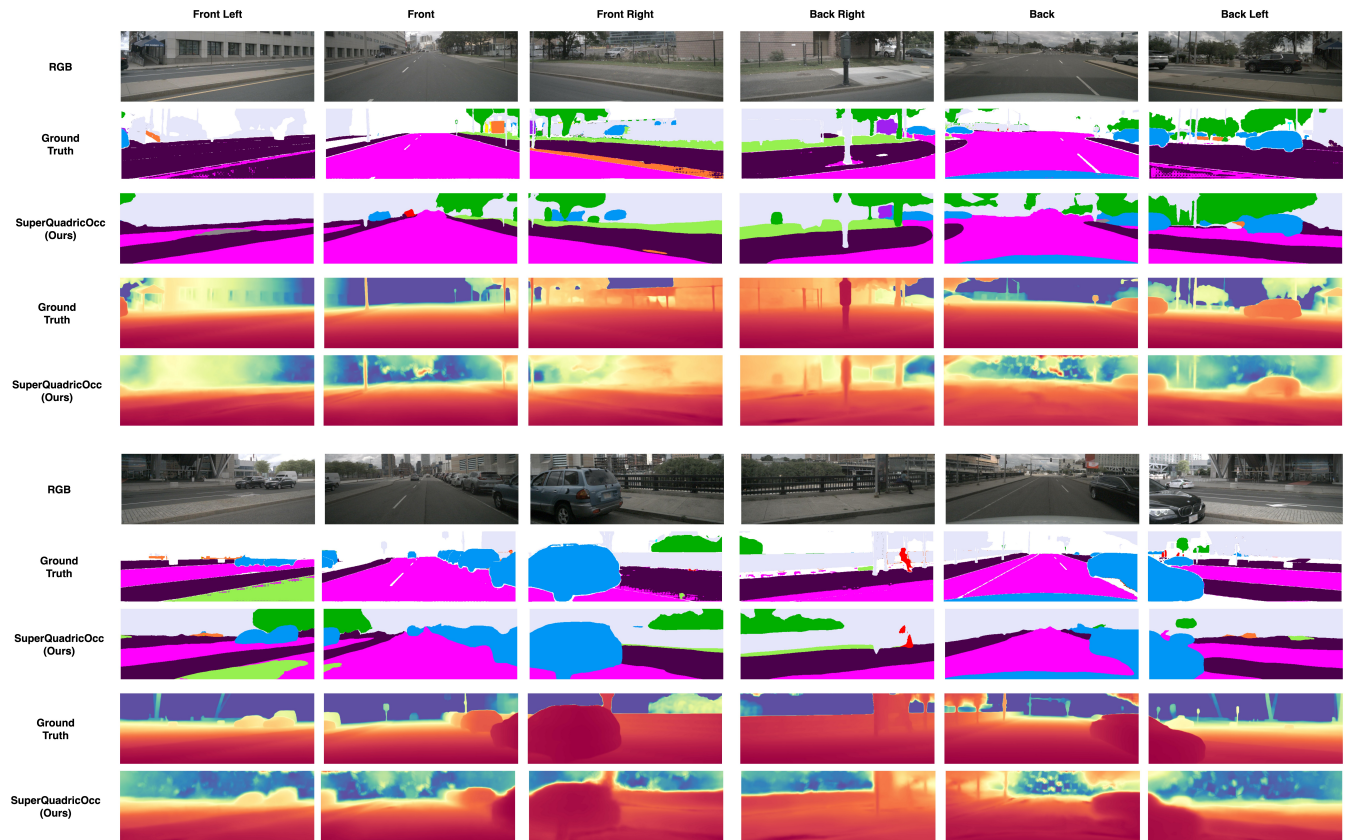


Fig. 7: **Depth and Semantics Visualized for SuperQuadricOcc:** For sample tokens a442b57b3e044dbcbce729bf3db01af36 and 4dfb0052fe944420acddf5d376755dff.

- [20] H. Caesar, V. Bankiti, A. H. Lang, S. Vora, V. E. Liong, Q. Xu, A. Krishnan, Y. Pan, G. Baldan, and O. Beijbom, "nusenes: A multimodal dataset for autonomous driving," in *2020 IEEE/CVF Conference on Computer Vision and Pattern Recognition (CVPR)*, 2020, pp. 11 618–11 628.
- [21] Y. Liao, J. Xie, and A. Geiger, "Kitti-360: A novel dataset and benchmarks for urban scene understanding in 2d and 3d," *IEEE Transactions on Pattern Analysis and Machine Intelligence*, vol. 45, no. 3, pp. 3292–3310, 2022.
- [22] Z. Li, W. Wang, H. Li, E. Xie, C. Sima, T. Lu, Q. Yu, and J. Dai, "Bev-former: learning bird's-eye-view representation from lidar-camera via spatiotemporal transformers," *IEEE Transactions on Pattern Analysis and Machine Intelligence*, 2024.
- [23] Z. Yan, W. Dong, Y. Shao, Y. Lu, L. Haiyang, J. Liu, H. Wang, Z. Wang, Y. Wang, F. Remondino, and Y. Ma, "Renderworld: World model with self-supervised 3d label," 2025. [Online]. Available: <https://arxiv.org/abs/2409.11356>
- [24] Z. Ming, J. S. Berrio, M. Shan, and S. Worrall, "Occfusion: Multi-sensor fusion framework for 3d semantic occupancy prediction," *IEEE Transactions on Intelligent Vehicles*, 2024.
- [25] Y. Wang, Y. Chen, X. Liao, L. Fan, and Z. Zhang, "Panoocc: Unified occupancy representation for camera-based 3d panoptic segmentation," in *Proceedings of the IEEE/CVF conference on computer vision and pattern recognition*, 2024, pp. 17 158–17 168.
- [26] Y. Wu, Z. Yan, Z. Wang, X. Li, L. Hui, and J. Yang, "Deep height decoupling for precise vision-based 3d occupancy prediction," in *2025 IEEE International Conference on Robotics and Automation (ICRA)*. IEEE, 2025, pp. 12 647–12 654.
- [27] Z. Ming, J. S. Berrio, M. Shan, Y. Huang, H. Lyu, N. H. K. Tran, T.-Y. Tseng, and S. Worrall, "Occcylindrical: Multi-modal fusion with cylindrical representation for 3d semantic occupancy prediction," *arXiv preprint arXiv:2505.03284*, 2025.
- [28] Y. Lu, X. Zhu, T. Wang, and Y. Ma, "Octreeocc: Efficient and multi-granularity occupancy prediction using octree queries," *Advances in Neural Information Processing Systems*, vol. 37, pp. 79 618–79 641, 2024.
- [29] Y. Huang, W. Zheng, Y. Zhang, J. Zhou, and J. Lu, "Gaussianformer: Scene as gaussians for vision-based 3d semantic occupancy prediction," in *European Conference on Computer Vision*. Springer, 2024, pp. 376–393.
- [30] Y. Huang, A. Thammadatrakoon, W. Zheng, Y. Zhang, D. Du, and J. Lu, "Gaussianformer-2: Probabilistic gaussian superposition for efficient 3d occupancy prediction," in *Proceedings of the Computer Vision and Pattern Recognition Conference*, 2025, pp. 27 477–27 486.
- [31] S. Zuo, W. Zheng, Y. Huang, J. Zhou, and J. Lu, "Gaussianworld: Gaussian world model for streaming 3d occupancy prediction," in *Proceedings of the Computer Vision and Pattern Recognition Conference*, 2025, pp. 6772–6781.
- [32] L. Zhao, S. Wei, J. Hays, and L. Gan, "Gaussianformer3d: Multi-modal gaussian-based semantic occupancy prediction with 3d deformable attention," *arXiv preprint arXiv:2505.10685*, 2025.
- [33] J. Park, Y. Hu, C. Peng, W. Zheng, K. Kitani, and W. Zhan, "S2go: Streaming sparse gaussian occupancy prediction," *arXiv preprint arXiv:2506.05473*, 2025.
- [34] Y. Shi, Y. Zhu, S. Han, J. Jeong, A. Ansari, H. Cai, and F. Porikli, "Odg: Occupancy prediction using dual gaussians," *arXiv preprint arXiv:2506.09417*, 2025.
- [35] S. Xu, F. Li, S. Jiang, Z. Song, L. Liu, and Z. xin Yang, "Gaussianpretrain: A simple unified 3d gaussian representation for visual pre-training in autonomous driving," 2024. [Online]. Available: <https://arxiv.org/abs/2411.12452>
- [36] Q. Sun, C. Shu, S. Zhou, Z. Yu, Y. Chen, D. Yang, and Y. Chun, "Gsrender: Duplicated occupancy prediction via weakly supervised 3d gaussian splatting," *arXiv preprint arXiv:2412.14579*, 2024.
- [37] L. Lei, S. Xu, Y. Bai, and X. Wei, "Tacocc: Target-adaptive cross-modal fusion with volume rendering for 3d semantic occupancy," *arXiv preprint arXiv:2505.12693*, 2025.
- [38] L. Chambon, E. Zablocki, A. Boulch, M. Chen, and M. Cord, "Gaussrender: Learning 3d occupancy with gaussian rendering," in *Proceedings of the IEEE/CVF International Conference on Computer Vision*, 2025, pp. 27 010–27 020.
- [39] L. Barsellotti, L. Bianchi, N. Messina, F. Carrara, M. Cornia, L. Baraldi, F. Falchi, and R. Cucchiara, "Talking to dino: Bridging self-supervised vision backbones with language for open-vocabulary segmentation," *arXiv preprint arXiv:2411.19331*, 2024.
- [40] A. Radford, J. W. Kim, C. Hallacy, A. Ramesh, G. Goh, S. Agarwal, G. Sastry, A. Askell, P. Mishkin, J. Clark *et al.*, "Learning transferable visual models from natural language supervision," in *International conference on machine learning*. PmlR, 2021, pp. 8748–8763.
- [41] M. Oquab, T. Darcet, T. Moutakanni, H. Vo, M. Szafraniec, V. Khalidov, P. Fernandez, D. Haziza, F. Massa, A. El-Nouby *et al.*, "Dinov2: Learning robust visual features without supervision," *arXiv preprint arXiv:2304.07193*, 2023.
- [42] A. H. Barr, "Superquadrics and angle-preserving transformations," *IEEE Computer graphics and Applications*, vol. 1, no. 01, pp. 11–23, 1981.
- [43] S. Alaniz, M. Mancini, and Z. Akata, "Iterative superquadric recombination of 3d objects from multiple views," in *Proceedings of the IEEE/CVF International Conference on Computer Vision*, 2023, pp. 18 013–18 023.
- [44] Y. Zhang, *Superquadric representation of scenes from multi-view range data*. The University of Tennessee, 2003.
- [45] D. Paschalidou, A. O. Ulusoy, and A. Geiger, "Superquadrics revisited: Learning 3d shape parsing beyond cuboids," in *Proceedings of the IEEE/CVF conference on computer vision and pattern recognition*, 2019, pp. 10 344–10 353.
- [46] Z. Gao, R. Yi, Y. Huang, W. Chen, C. Zhu, and K. Xu, "Partgs: Learning part-aware 3d representations by fusing 2d gaussians and superquadrics," *arXiv preprint arXiv:2408.10789*, 2024.
- [47] S. Jiang, Q. Zhao, H. Rahmani, D. W. Soh, J. Liu, and N. Zhao, "Gaussianblock: Building part-aware compositional and editable 3d scene by primitives and gaussians," *arXiv preprint arXiv:2410.01535*, 2024.
- [48] E. Fedele, B. Sun, L. Guibas, M. Pollefeys, and F. Engelmann, "Superdec: 3d scene decomposition with superquadric primitives," *arXiv preprint arXiv:2504.00992*, 2025.
- [49] A. Guédon and V. Lepetit, "Sugar: Surface-aligned gaussian splatting for efficient 3d mesh reconstruction and high-quality mesh rendering," in *Proceedings of the IEEE/CVF Conference on Computer Vision and Pattern Recognition*, 2024, pp. 5354–5363.
- [50] J. Wacziarg, P. Borycki, S. Tadeja, J. Tabor, and P. Spurek, "Games: Mesh-based adapting and modification of gaussian splatting," *arXiv preprint arXiv:2402.01459*, 2024.
- [51] Y. Huang, W. Zheng, B. Zhang, J. Zhou, and J. Lu, "Selfocc: Self-supervised vision-based 3d occupancy prediction," in *Proceedings of the IEEE/CVF conference on computer vision and pattern recognition*, 2024, pp. 19 946–19 956.
- [52] P. Tang, Z. Wang, G. Wang, J. Zheng, X. Ren, B. Feng, and C. Ma, "Sparseocc: Rethinking sparse latent representation for vision-based semantic occupancy prediction," in *Proceedings of the IEEE/CVF Conference on Computer Vision and Pattern Recognition*, 2024, pp. 15 035–15 044.